Synthesis and Characterization of Novel Poly(*o*-toluidine) Montmorillonite Nanocomposites: Effect of Surfactant on Intercalation

Rahul Singhal, Monika Datta

Analytical Research laboratory, Department of Chemistry, University of Delhi, Delhi 110007, India

Received 19 October 2006; accepted 25 March 2007
DOI 10.1002/app.26708
Published online 20 July 2007 in Wiley InterScience (www.interscience.wiley.com).

ABSTRACT: The investigation of clay based polymer nanocomposites has opened the door for the development of novel, ecofriendly advanced nano materials that can be safely recycled. Because of their nanometer size dispersion, these nanocomposites often have superior physical and mechanical properties. In this study, novel nanocomposites of poly(*o*-toluidine) (POT) and organically modified montmorillonite (MMT) were synthesized using camphor sulfonic acid (CSA), cetyl pyridinum chloride (CPCl), and *N*-cetyl-*N*,*N*,*N*-trimethyl ammonium bromide (CTAB) to study the role of surfactant modification on the intercalation. The in situ intercalative polymerization of POT within the organically modified MMT layers was analyzed by FTIR, UV–visible, XRD, SEM as well as TEM studies. The average particle size of the nanocomposites was found to be in the range 80–100 nm. © 2007 Wiley Periodicals, Inc. J Appl Polym Sci 106: 1909–1916, 2007

Key words: montmorillonite; nanocomposite; poly(*o*-toluidine); morphology; intercalation; surfactants

INTRODUCTION

Nanotechnology has been recognized as one of the most promising areas for technological advancement in the 21st century. The development of polymer nanocomposites is an emerging field of research, which has led to the enhancement of material properties via interfacial interaction between the polymer matrix and the organically modified layered silicates.[1–5] It has been lately investigated that the ground state of polymer–clay nanocomposites corresponds to phase-separated, intercalated, or exfoliated depending on the external conditions. Hence, the mechanism of structural transitions between such states has become a subject of great scientific and practical importance. Intercalation polymerization is a promising technique that has resulted in the fabrication of several polymer nanocomposite materials. Conducting polymer intercalated nanocomposites prepared by this method lead to higher degree of polymer ordering resulting in advanced gas barrier, thermal, electrical as well as mechanical properties.[6–11] Many published papers focusing on the preparation and new properties of novel nanocomposites containing conducting polymers particularly polyaniline (PANI) with various host materials such as FeOCl,[12] MoO_3,[13] V_2O_5[14] have been reported.

One of the most studied pairs in conducting polymer/layered inorganic solid nanocomposites are the nanocomposites composed of PANI chains confined in the 2-D galleries of layered silicates with the unique characteristics mentioned above. After the observation of PANI intercalation into Cu^{2+}-exchanged silicates by Cloos et al. in 1979,[15] a number of studies on the preparation, properties, and applications of PANI/layered silicate nanocomposites were carried out.[16–22] Most recently, Yang and Chen[23] reported the synthesis of PANI/organically modified clay nanocomposites and found that more ordered PANI chains were formed between interlayer spacings of the modified clay, especially for $HOOC(CH_2)_{11}NH_{31}$ modified clay. Because the acidic $HOOC(CH_2)_{11}NH_{31}$ ions residing between interlayer spacings provide a stronger driving force for the intercalation of aniline monomer. Yeh et al.[24] reported the synthesis of PANI/clay nanocomposites with exfoliated silicate layers of clay and investigated the effect of such nanocomposites on the corrosion protection of cold rolled steel (CRS) when compared with that of an emeraldine base of PANI using a series of electrochemical measurements of corrosion potential and polarization resistance. However, the study of the complex structure of the nanocomposites and the confinement of the polymer chains in the silicate galleries, still remains an unambiguous problem that needs to be further resolved.

Our earlier results based on PANI/bentonite nanocomposites have shown that lower extent of intercalation of PANI takes place in the bentonite galleries as

Correspondence to: Monika Datta (monikadatta_chem@yahoo.co.in).

compared with the reported PANI/MMT nanocomposites and the particle size of the nanocomposites was found to be on the higher side of the nanometer range.[25] In the present study, we have chosen montmorillonite (MMT) as a host material, because its layered structure consists of two silica tetrahedral sheets held together by weak dipolar forces in which the monomer can be easily introduced by ion exchange without distorting its layered morphology. The surfactant modification of MMT was carried out, as the long chain alkyl ammonium salts or surfactants helps to facilitate the interaction between MMT and polymer chains by making the hydrophilic MMT surface organophilic without distorting the layered structure, which helps in improving the compatibility between the silicate layers and polymer. Moreover, as the understanding of PANI/silicate nanocomposites is fragmentary owing to the amorphous nature of PANI as well as its low solubility in common organic solvents, poly(*o*-toluidine) (POT) was chosen as the conducting polymer owing to its higher processibility as well as solubility as compared with PANI.[25]

To the best of our knowledge, systematic studies on the effect of cationic and anionic surfactants on the physical properties of POT/MMT nanocomposites are not reported in literature. The present work reports preliminary investigations on the synthesis and characterization of POT/MMT nanocomposites using cationic as well as anionic surfactants. The effect of surfactant on the intercalation, spectral, and morphological properties of the nanocomposites was investigated.

EXPERIMENTAL

Materials

Montmorilonite Clay obtained from Adrich, Chemical Co. was used for synthesis. *o*-Toluidine (Aldrich, AR) was distilled twice under reduced pressure prior to use Potassium persulphate (Aldrich, AR), *N*-cetyl-*N*,*N*,*N*-trimethyl ammonium bromide (CTAB) (Aldrich, AR), cetyl pyridinuim chloride(Aldrich, AR), D-10 camphorsulphonic acid (Aldrich, AR), dodecylbenzenesulphonic acid (Aldrich, AR), HCl (GR, Merck, India) were used as such without further purification.

Modification of MMT clay

MMT was organically modified with the surfactants before it was intercalated with the monomer (*o*-toluidine). A known amount of clay (2 g) 25 mL of each of them were mixed with $\sim 0.1M$ of surfactant and then kept for stirring for 3 h using magnetic stirrer. It was than centrifuged and washed several times with distilled water to remove excess of surfactant after, then dried in vacuum oven at 80°C (Table I).

TABLE I
Recipe for Modification of MMT and Synthesis of POT/MMT Nanocomposites

Material	Surfactant (g) (0.1*M*)	Monomer (g)	Yield (%)
MMT (CTAB)	0.9	–	78
MMT (CPC)	0.89	–	75
MMT (CSA)	0.58	–	80
POT/MMT (CTAB)	0.9	1	83
POT/MMT (CPC)	0.89	1	85
POT/MMT (CSA)	0.58	1	90

Synthesis of poly(*o*-toluidine)–MMT nanocomposites

A measured volume of freshly distilled toluidine (1 mL) was syringed slow into a modified clay (0.5 g). To this ammonium persulphate (0.268 g) was added followed by 40 mL of distilled water and to this 2–3 drops of HCl was added at 0°C. The gradual change of color from gray to dark purple was indicative of the formation of POT. After 4 h of constant stirring, the total mass was centrifuged and the residue was washed with distilled water. The nanocomposite obtained was dried under vacuum at 80°C for 24 h, to obtain the intense black colored nanocomposite powder (Table I).

Characterization

FTIR spectra of the nanocomposites were taken on a spectrometer model IMPACT 410, NICOLET. UV–visible spectra were taken on Perkin–Elmer lambda EZ-221. X-ray diffractograms were recorded on X-ray diffractometer model Philips PW3710 using copper Kα radiations. TEM was taken on Morgagni 268-D TEM FEI, Netherlands. Scanning electron micrographs were taken on JEOL JSM840 scanning electron microscope under gold film.

RESULTS AND DISCUSSION

Characteristics of modified MMT and POT intercalated MMT

The percent yield of organically modified MMT (Fig. 1) was found to be higher for MMT(CTAB) and MMT (CSA), while it was found to be lower for MMT(CPCl), which can be attributed higher ionic interaction incase of CTAB and CSA with MMT than CPCl. The percent yield of polymer modified MMT (Fig. 2) was found to be around 80–90% for POT/MMT(CSA), POT/MMT(CTAB), and POT/MMT(CPCl). The polymerization of POT was confirmed by the instant color change to dark purple upon addition of *o*-toluidine. It has been reported that the chemical composition of MMT has a catalytic effect on the polymerization[21] and similar phenomenon was observed in our case.

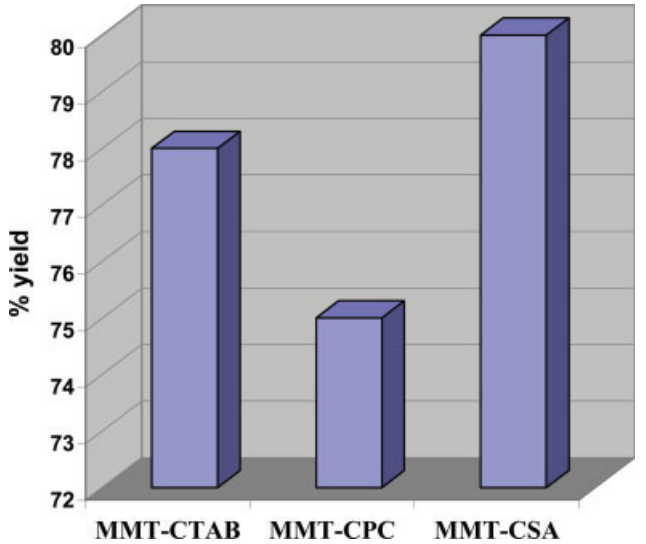

Figure 1 % yield of surfactant modified MMT. [Color figure can be viewed in the online issue, which is available at www.interscience.wiley.com.]

Because the negative charge originates from the silicate layer, the cationic head group of the surfactant molecule preferentially resides at the layer surface, while the aliphatic tail is removed from the surface. The presence of these aliphatic chains in the galleries modifies the original hydrophilic silicate surface to be organophilic. Furthermore, the organic cations contain various functional groups that react with the polymers and reinforce adhesion between the particles and the matrix, thus producing nanocomposites with excellent dispersion quality in organic solvents. As the surfactant chain length gets larger, the charge density of the clay increases, which influences the percentage yield.

FTIR spectra

The FTIR spectra of MMT clay [Fig. 3(a)], shows the characteristic absorption peaks of lattice water (O-H) at 3267 cm^{-1}, 3400 cm^{-1}, CH_2 asymmetric stretching vibrations (C-H) at 2360 cm^{-1}, H-O-H bending (H-O-H) and Si-O stretching vibrations at 1638, 1054, and 1106 cm^{-1}, respectively. In case of surfactant modified MMT prepared by modification with CSA, CTAB, and CPCl [Fig. 3(b–d)], the OH stretching, H-O-H bending, Si-O bending peaks show a major shift of 9 cm^{-1} from 1054 to 1045 cm^{-1} in CTAB/MMT, CPCl/MMT, and CSA/MMT thus confirming the organic modification of the clay via the surfactants (Table I). Likewise the HOH bending peak also shows a shift of 7 cm^{-1} incase of CTAB/MMT and CPCl/MMT, while it shows a shift of 2 cm^{-1} incase of CSA/MMT. The shifting of Si-O as well as H-O-H bending peak indicates the organic modification of MMT via ionic interaction of the clay with surfactants. In case of polymer intercalated surfactant modified MMT, shifting of the characteristic peaks of Si-O and H-O-H bending by 9 cm^{-1} is noticed for POT/MMT(CTAB), POT/MMT(CSA), and POT/MMT(CPCL), while additional peaks corresponding to benzenoid and quinonoid vibrations are observed at 1489 cm^{-1} [Fig. 3(e–g)], thus confirming the polymerization of toluidine within the organically modified galleries of MMT.[26]

UV–visible spectra

The UV–visible spectra of POT/MMT (CTAB) (Fig. 4) shows broad absorption maximas at 350 and 550 nm. The peak in the UV range is assigned to Π–Π* transitions, whereas the peak in the visible range is assigned to the polaronic transitions from the benzenoid ring (HUMO) to the quinonoid ring (LOMO), i.e., from Π_B–Π_Q. The peak in the visible range also confirms the presence of the doped state of conducting polymer (POT) in MMT.[27] Incase of POT/MMT(CTAB), a free carrier tail is observed in the visible region, which is consistent with the delocalization of polarons promoted by extended chain conformation of POT and has also been observed for PANI.[28] Incase of POT/MMT(CSA) and POT/MMT(CPCl), the transitions in the visible range transitions appear to be well formed and localized exhibiting a compact coil conformation of POT.[27] The strong interactions between the POT chains incase of POT/MMT(CPCl) and POT/MMT(CSA) make conjugation defects leading to a compact coil conformation, while incase of

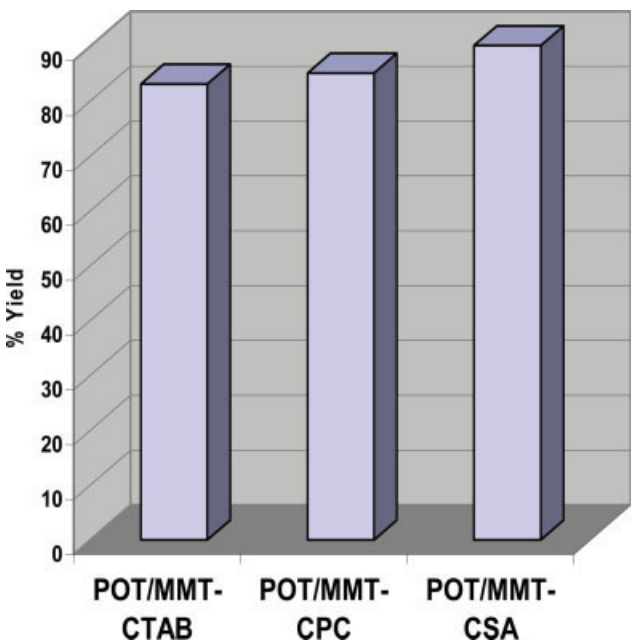

Figure 2 % yield of POT/MMT. [Color figure can be viewed in the online issue, which is available at www.interscience.wiley.com.]

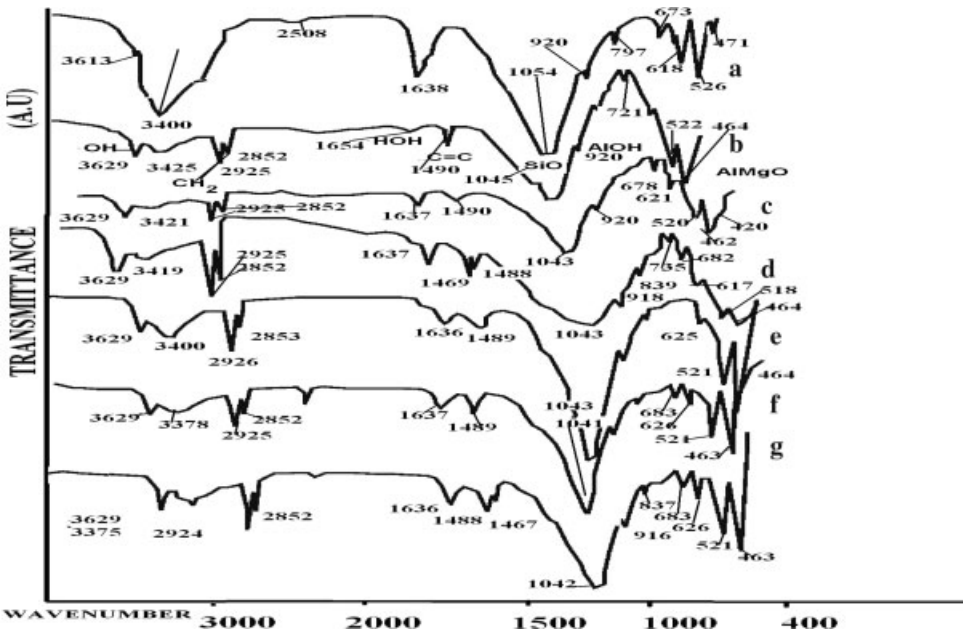

Figure 3 FTIR spectra of (a) MMT, (b) MMT(CTAB), (c) MMT(CPCl), (d) MMT(CSA), (e) POT/MMT(CTAB), (f) POT/MMT(CPCl), (g) POT/MMT(CSA).

POT/MMT(CTAB), the stacking of POT chains in between the MMT layer tends to eliminate the interaction between the POT chains leading to dispersed polaron band, which appears as a free carrier tail in the spectra. Thus, it can be concluded that the surfactant modification of MMT leads to different chain conformations of POT within the MMT galleries exhibiting an expanded structure in POT/MMT(CTAB) and a compact coil structure in POT/MMT(CPCl) as well as POT/MMT(CSA).[27]

XRD analysis

The (001) reflection peak of the pristine MMT is observed around $2\theta \sim 7.34^\circ$ for [Fig. 5(a)] 12 Å. In case of polymer clay nanocomposites, the corresponding shift of the (001) diffraction peak towards lower angles indicates an increase in the inter gallery spacing. The observed expansion of the clay gallery reflects the extent of intercalation. The modification of MMT with CTAB [Fig. 5(b)] shows an increase in the height of the gallery from 12 to 13.8 Å, while that of POT/MMT(CTAB) shows an increase up to 14.4 Å

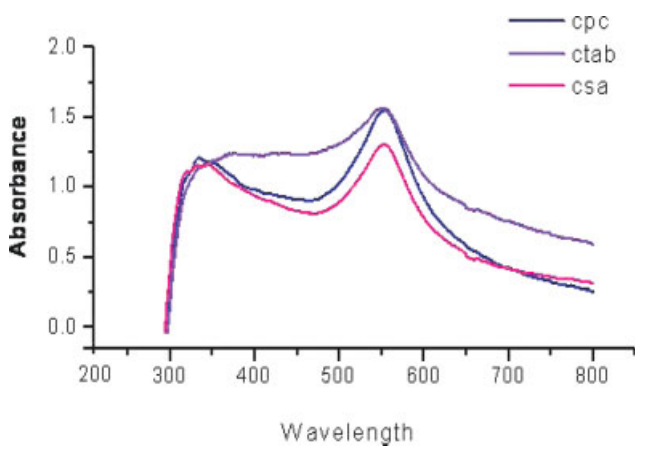

Figure 4 UV–visible spectra of POT/MMT nanocomposites. [Color figure can be viewed in the online issue, which is available at www.interscience.wiley.com.]

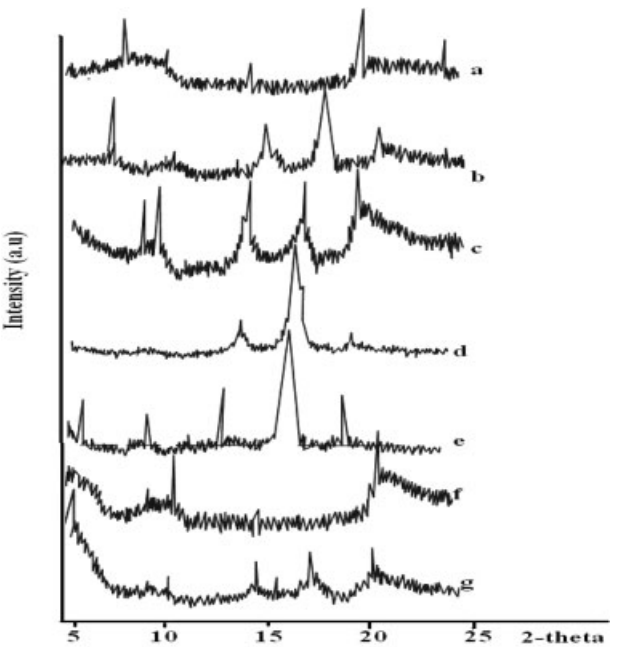

Figure 5 XRD Spectra of (a) MMT, (b) MMT(CTAB), (c) MMT(CPCl), (d) MMT(CSA), (e) POT/MMT(CTAB), (f) POT/MMT(CPCl), (g) POT/MMT(CSA).

TABLE II
X-ray *d*-Spacings of MMT, Surfactant Modified MMT and POT Intercalated Organically Modified MMT

S. no	Sample	Diffraction angle (2θ)	*d*-spacing (0A)	Increase in *d*-spacing (0A)
1	MMT	7.345	12	–
2	MMT (CTAB modified)	6.375	13.8	1.8
4	MMT (CSA modified)	–	–	–
5	MMT (CPC modified)	–	–	–
6	POT/MMT (CTAB)	6.110	14.45	2.45
7	POT/MMT (CSA)	5.210	16.94	4.94
8	POT/MMT (CPC)	–	–	–
9	PANI/MMT[29]	5.9	14.8	5.2
10	PEOA/MMT[30]	–	–	3.9

probably due to the transition of POT from the ''compact coil'' to an ''expanded coil'' indicating the possibility of more expanded conformation of POT chains as well as its successful intercalation. The CSA modified MMT [Fig. 5(c)] exhibits exfoliation while POT/MMT(CSA) [Fig. 5(d)] reveals an expansion of intergallery spacing by 4 Å indicating the presence of an expanded coil conformation of POT in the MMT galleries. The 001 diffraction peak appears to be absent in CPCl modified MMT [Fig. 5(e)] as well as POT/MMT(CPCl) [Fig 5(f)] indicating that either destruction of the interlayer (001) spacing takes place upon modification with CPCl or higher increase in the intergallery spacing takes place, which shifts the 001 diffraction peaks to values lower than 5 Å.[28] As the intergallery spacing remains intact for 002 spacing it can be ruled out that complete exfoliation of modified clay or nanocomposite does not takes place but higher intercalation occurs, which shifts the diffraction peaks to much lower values. As compared with the reported values for PANI/MMT[29] and polyethoxyaniline/MMT,[30] we notice that in our case higher expansion in the *d*-spacing is observed (Table II), which confirms greater intercalation of POT in MMT galleries.

It can be concluded that the pure organo clay interlayer spacing increases with longer surfactant chain length and with higher surfactant concentration on the clay surface, which further increases after POT chain insertion.

The percent increase in the gallery spacing (Fig. 6) reveals that 16% intercalation takes place in the CTAB modified MMT, while exfoliation is observed for CPCl and CSA modified MMT. However, incase of POT/MMT (Fig. 7) 20 and 45% intercalation is observed for POT/MMT(CTAB) and POT/MMT(CSA), respectively, while exfoliation is observed for POT/MMT(CPCl).

TEM studies

The TEM micrograph of MMT shows the presence of nearly spherical globular MMT particles [Fig. 8(a)]

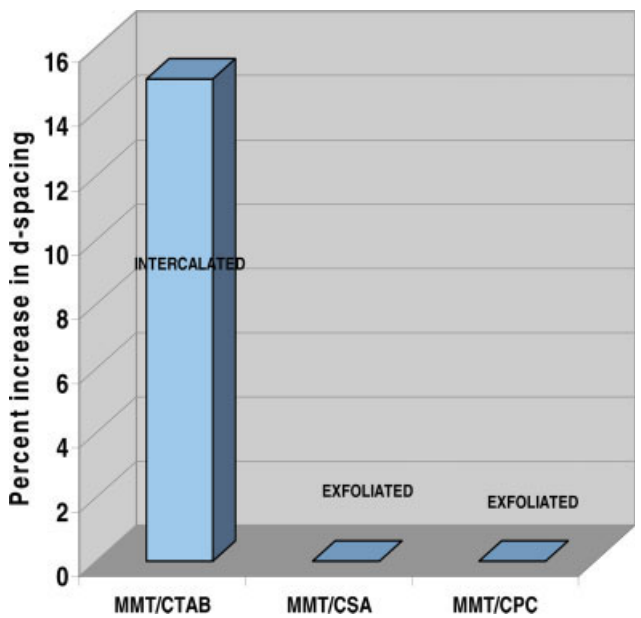

Figure 6 % Intercalation of Surfactant in MMT. [Color figure can be viewed in the online issue, which is available at www.interscience.wiley.com.]

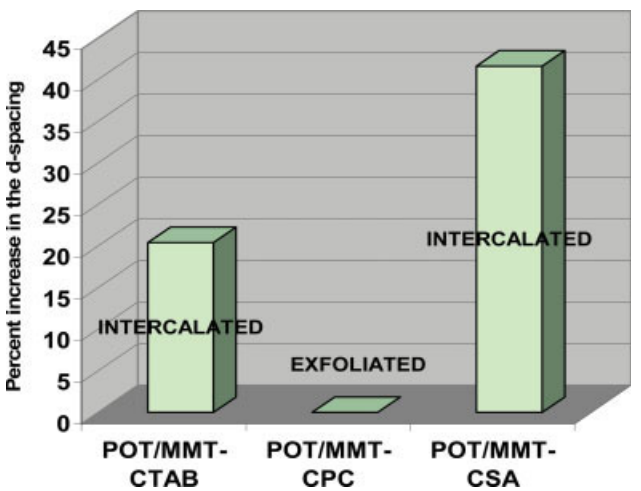

Figure 7 % Intercalation of POT in MMT. [Color figure can be viewed in the online issue, which is available at www.interscience.wiley.com.]

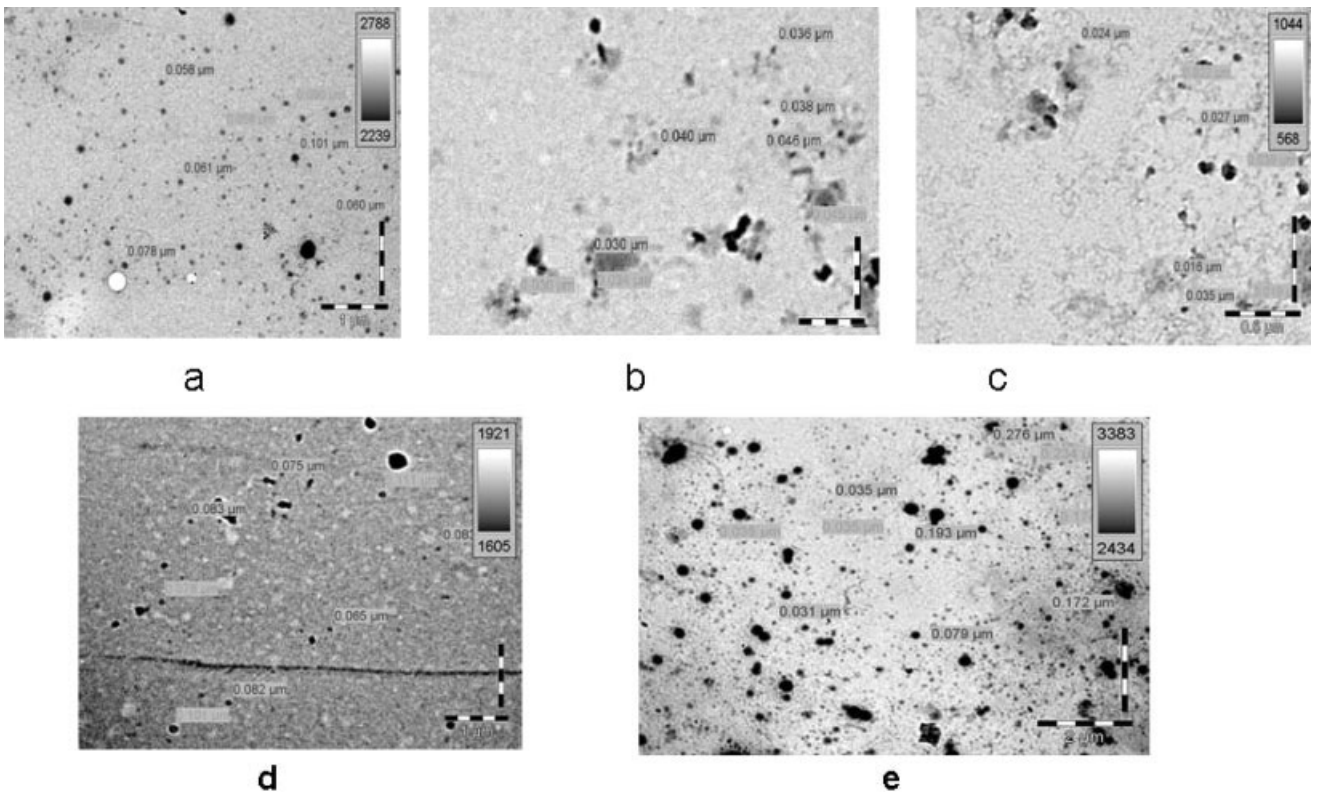

Figure 8 TEM micrographs of (a) MMT, (b) MMT(CTAB), (c) POT/MMT(CTAB), (d) MMT(CSA), (e) POT/MMT(CSA).

that appear to be dispersed. The morphology reveals uniform distribution of MMT particles. The average diameter of the particles is found to be in the range of 60–100 nm, which is reported by some authors as well.[31] The particles are characterized by a typical raspberry morphology, where the minute silica particles tend to be distributed throughout the agglomerates.[31] Upon modification with surfactant, we find that the particles size of the modified clay decreases immensely. The TEM micrograph of MMT/CTAB [Fig. 8(b)] reveals a nearly granular morphology and the aggregate size are found to be in the range 30–40 nm. The micrograph reveals nonuniform distribution of small particles. The TEM image of POT/MMT(CTAB) nanocomposite [Fig. 8(c)] shows even smaller particle sizes of 30–35 nm that have an extremely uniform distribution as well as particle size. The TEM micrograph of MMT(CSA) [Fig. 8(d)], however, shows large dense aggregates distributed uniformly throughout the MMT clay particles having an average cluster size of 60–80 nm. However the POT/MMT(CSA) [Fig. 8(e)] shows fine uniform distribution of particles having a dense spherical aggregates of 100 nm in size. The particle size is found to be lower than the reported PANI/MMT and PEOA/MMT nanocomposites.[29,30]

Hence it can be concluded that the internal structure of the nanocomposites is strongly influenced by the clay structure and the intercalated polymer. In our case uniform morphology as well as smaller particles size is obtained incase of all the POT/MMT nanocomposites exhibiting a well intercalated polymer/clay structure as confirmed by UV as well as XRD analysis.

SEM analysis

The SEM micrograph of MMT [Fig. 9(a)] exhibits clusters of fine clay particles. Upon surfactant modification, MMT shows a dramatic improvement in the morphology of the clay particles. The SEM micrograph of MMT/CTAB [Fig. 9(b)] reveals a rough granular morphology showing large loosely packed fused grains forming fluffy agglomerates while SEM micrograph of POT/MMT(CTAB) [Fig. 9(c)] reveals bright flaky aggregates that are densely packed. The SEM micrograph of MMT/CSA [Fig. 9(d)] shows the presence of an uneven layered structure forming intimate, dense, and granular agglomerate. However, the morphology of POT/MMT(CSA) [Fig. 9(e)] exhibits the formation of a fused well organized layered morphology having flaky structures.

It can be concluded that the variation of morphology of the nanocomposites, is predominantly governed by the nature of the oxidant used, which influences conformation of POT chains in the MMT layers.

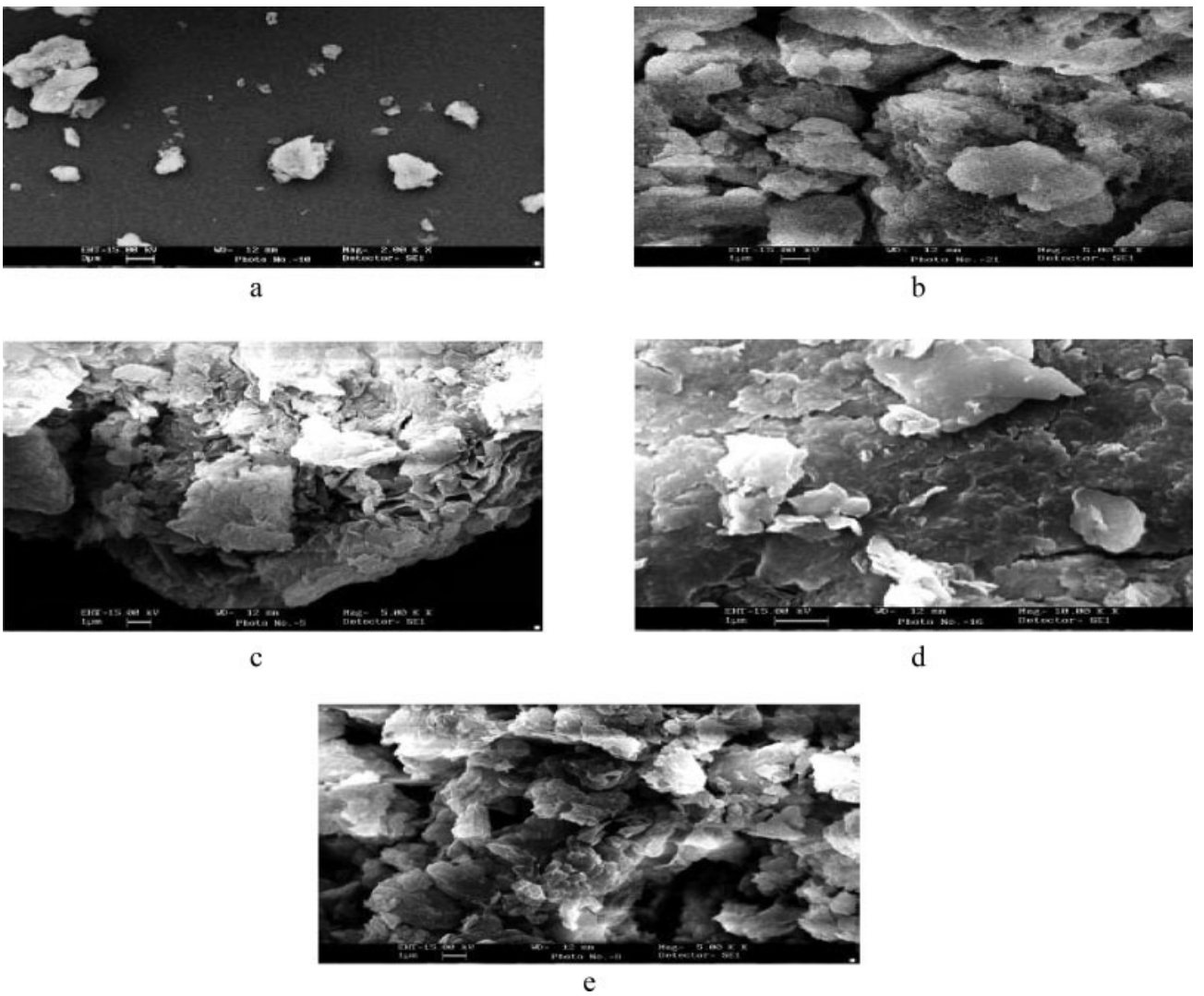

Figure 9 SEM micrographs of (a) MMT, (b) MMT(CTAB), (c) POT/MMT(CTAB), (d) MMT(CSA), (e) POT/MMT(CSA).

CONCLUSIONS

Nanocomposites of MMT with POT were successfully synthesized. FTIR spectra confirmed the possible interaction between MMT and anionic, cationic surfactants as well as polymerization of POT in the MMT galleries. The XRD as well as morphological results inferred that modification of MMT as well as intercalation of POT into the MMT galleries was found to be dependent of the alkyl chain length, size, and charge of the surfactant. Uniform, intimately packed, layered morphologies were obtained in case of POT/MMT nanocomposites. The control drug release studies by these nanocomposites are in progress in our laboratory and will be published soon.

The authors thank Dr. S.P. Singh Scientist C at National Physical Laboratory, Delhi for interpreting the UV–visible spectra and Bahavan Gera for her assistance in carrying out the experimental procedure. The authors also acknowledge the sophisticated analytical instrumentation facility (S.A.I.F) at All Indian Institute of Medical Sciences (A.I.I.M.S) for carrying out the TEM as well as SEM analysis.

References

1. Ray, S. S.; Okamoto, M. Prog Polym Sci 2003, 28, 1539.
2. Jeon, H. G.; Jung, H. T.; Lee, S. W.; Hudson, S. D. Polym Bull 1998, 41, 107.
3. Tian, Y.; Yu, H.; Wu, S.; Ji, G. J. Mater Sci 2004, 39, 4301.
4. Kuan, H. C.; Chuang, W. P.; Ma, C. M.; Chiang, C. L.; Wu, H. L. J Mater Sci 2005, 40, 179.
5. Yano, K.; Usuki, A.; Okada, A. Polym Sci A Polym Chem 1997, 35, 2289.
6. Choi, H. J.; Kim, S. G.; Hyun, Y. H.; Jhon, M. S. Macromol Rapid Commun 2001, 22, 320.
7. Galgali, G.; Ramesh, C.; Lele, A. Macromolecules 2001, 34, 852.
8. Yonezawa, S.; Kanamura, K.; Takehara, Z. J Electrochem Soc 1993, 140, 629.
9. Palmisano, F.; De Benedetto, G. E.; Zambonin, C. G. Analyst 1997, 122, 365.

10. Anuar, K.; Abdullah, A. H.; Idris, Z. Ultra Sci 2001, 12, 2.
11. Yoshino, K. Synth Metals 1989, 28, 669.
12. Kerr, T. A.; Wu, H.; Nazar, L. F. Chem Mater 1996, 8, 2005.
13. Wu, C. G.; DeGroot, D. C.; Marcy, H. O.; Schindler, J. L.; Kannewurf, C. R.; Bakas, T; Hirpo, W.; Yesinoswki, J. P.; Liu, Y. J.; Kanatzidis, M. G. J Am Chem Soc 1995, 117, 9229.
14. Wu, C. G.; Liu, Y. C.; Hsu, S. S.; Li, C. Synth Metals 1999, 102, 1268.
15. Mehrotra, V.; Giannelis, E. P. Solid State Ionics 1992, 51, 115.
16. Chang, T.-C.; Ho, S.-Y.; Chao, K.-J. J Chin Chem Soc 1992, 39, 209.
17. Wu, Q.; Xue, Z.; Qi, Z.; Wang, F. Polymer 2000, 2029, 41.
18. Kim, J. W.; Kim, S. G.; Choi, H. J.; Jhon, M. S. Macromol Rapid Commun 1999, 20, 450.
19. Cloos, P.; Moreale, A.; Braers, C.; Badot, C. Clay Miner 1979, 14, 307.
20. Inoue, H.; Yoneyama, H. J Electroanal Chem 1987, 233, 291.
21. Jia, W.; Segal, E.; Kormandel, D.; Lamhot, Y.; Narkis, M.; Siegmann, A. Synth Metals 2002, 128, 115.
22. Mizoguchi, K.; Kim, J. W.; Choi, H. J. Macromolecules 2002, 35, 1419.
23. Yang, S. M.; Chen, K. H. Synth Metals 2003, 51, 135.
24. Yeh, J.-M.; Liou, S.-J.; Lai C.-Y.; Wu, P.-C. Chem Mater 2001, 13, 1131.
25. Datta, M.; Singhal, R. J Appl Polym Sci 2006, 103, 3299.
26. Bilal, S.; Holze, R. J Electroanal Chem 2006, 592, 1.
27. Wu, Q.; Xue, Z.; Qi, Z.; Wang, F. Polymer 2005, 41, 2032.
28. Ashraf, S. M.; Ahmad, S.; Riaz, U. J Macromol Sci Part B: Macromol Phys 2006, 45, 1109.
29. Yoshimoto, S.; Ohashi, F.; Ohnishi, Y.; Nonami, T. Synth Metals 2001, 145, 265.
30. Choi, J. S.; Sung, J. H.; Choi, H. J.; Jhon, M. S. Synth Metals 2005, 153, 129.
31. Biswas, M.; Ray, S. S. J Appl Polym Sci 2000, 77, 2948.